by the other methods were not in complete agreement is ascribed to the complex sequence of steps occurring during the former. The correlation between long-term shelf stability of emulsions and their resistance to high-speed centrifugation was not sufficiently good to make the latter a reliable technique for predicting the former (32, 33).

REFERENCES

(1) H. Schott, *J. Colloid Interface Sci.*, **43**, 150 (1973).

(2) H. Schott and S. K. Han, *J. Pharm. Sci.*, **64**, 658 (1975).

(3) W. N. Maclay, *J. Colloid Sci.*, **11**, 272 (1956).

(4) M. J. Schick, *J. Colloid Sci.*, **17**, 801 (1962).

(5) H. Schott and S. K. Han, *J. Pharm. Sci.*, **66**, 165 (1977).

(6) M. J. Schick and A. H. Gilbert, *J. Colloid Sci.*, **20**, 464 (1965).

(7) H. Schott and S. K. Han, *J. Pharm. Sci.*, **65**, 975 (1976).

(8) H. Schott and A. E. Royce, *J. Pharm. Sci.*, **72**, 313 (1983).

(9) G. Herdan, "Small Particle Statistics," 2nd ed., Academic, New York, N.Y., 1960, chap. 4.

(10) K. J. Mysels, "Introduction to Colloid Chemistry," Interscience, New York, N.Y., 1959, chaps. 3 and 20.

(11) H. C. van de Hulst, "Light Scattering by Small Particles," Wiley, New York, N.Y., 1957, chaps. 10, 18, and 19.

(12) W. J. Youden, "Statistical Methods for Chemists," Wiley, New York, N.Y., 1951, chap. 5.

(13) G. F. Lothian and F. P. Chappel, *J. Appl. Chem.*, **1**, 475 (1951).

(14) J. D. S. Goulden, *Trans. Faraday Soc.*, **54**, 941 (1958).

(15) R. D. Vold and M. Maletic, *J. Colloid Interface Sci.*, **65**, 390 (1978), and 7 references cited therein.

(16) R. D. Vold and K. L. Mittal, *J. Soc. Cosmet. Chem.*, **23**, 171 (1972).

(17) R. D. Vold and R. C. Groot, *J. Soc. Cosmet. Chem.*, **14**, 233 (1963).

(18) T. Sato and R. Ruch, "Stabilization of Colloidal Dispersions by Polymer Adsorption," Dekker, New York, N.Y., 1980, chap. 3.

(19) P. H. Elworthy and A. T. Florence, *J. Pharm. Pharmacol.*, **21**, 70s (1969).

(20) P. H. Elworthy and A. T. Florence, *J. Pharm. Pharmacol.*, **21**, 79s (1969).

(21) M. J. Schick, S. M. Atlas, and F. R. Eirich, *J. Phys. Chem.*, **66**, 1326 (1962).

(22) L. Hsiao, H. N. Dunning, and P. B. Lorenz, *J. Phys. Chem.*, **60**, 657 (1956).

(23) P. H. Elworthy, A. T. Florence, and J. A. Rogers, *J. Colloid Interface Sci.*, **35**, 23 (1971).

(24) F. E. Bailey and R. W. Callard, *J. Appl. Polymer Sci.*, **1**, 56 (1959).

(25) A. T. Florence, F. Madsen, and F. Puisieux, *J. Pharm. Pharmacol.*, **27**, 385 (1975).

(26) S. Friberg, P. O. Jansson, and E. Cederberg, *J. Colloid Interface Sci.*, **55**, 614 (1976).

(27) E. H. Crook, D. B. Fordyce, and G. F. Trebbi, *J. Phys. Chem.*, **67**, 1987 (1963).

(28) R. D. Vold and R. C. Groot, *J. Phys. Chem.*, **66**, 1969 (1962).

(29) A. U. Hahn and K. L. Mittal, *Colloid Polymer Sci.*, **257**, 959 (1979).

(30) E. R. Garrett, *J. Soc. Cosmet. Chem.*, **21**, 393 (1970), and 3 references cited therein.

(31) S. J. Rehfeld, *J. Colloid Interface Sci.*, **46**, 448 (1974), and 1 reference cited therein.

(32) P. Sherman, *Soap Perfum. Cosmet.*, **44**, 693 (1971).

(33) R. D. Vold and M. C. Acevedo, *J. Am. Oil Chem. Soc.*, **54**, 84 (1977).

ACKNOWLEDGMENTS

Support by the National Institutes of Health under Grant GM 27802 is gratefully acknowledged.

X-ray Structural Studies and Physicochemical Properties of Cimetidine Polymorphism

MEGUMI SHIBATA ˣ, HIROMASA KOKUBO, KAZUHIRO MORIMOTO, KATSUAKI MORISAKA, TOSHIMASA ISHIDA, and MASATOSHI INOUE

Received April 2, 1982, from the *Osaka College of Pharmacy, 2-10-65 Kawai, Matsubara-City, Osaka 580, Japan.* Accepted for publication October 7, 1982.

Abstract □ Four crystalline forms of cimetidine, three anhydrous (forms A, B, and D) and a monohydrate (form C), obtained by slow evaporation of aqueous solutions of varying concentrations were characterized by IR spectroscopy, X-ray powder patterns, dissolution rates in deionized water, and thermal analyses. Among the three anhydrous forms of cimetidine, form A was thermodynamically more stable than the others. The structural conversion of form C into form A on dehydration was confirmed by IR spectroscopy and X-ray powder patterns. The structures of forms C and D were determined using X-ray diffraction. Form D was of spirally curled conformation; it was linked in a head-to-tail arrangement with the neighboring molecules *via* intermolecular hydrogen bonds between the imidazole nitrogen and guanidine nitrogen atoms. Form C was characterized by its folded conformation due to the weak stacking interaction between the imidazole and guanidine moieties; there was stabilization by double hydrogen bond formation with neighboring molecules and *via* water molecules of crystallization. The dissolution rate constant in deionized water for form C was ~1.29, 1.70, and 1.90 times greater than those measured for forms A, D, and B, respectively. There was a similar relationship among the four forms with respect to the rates of inhibition of stress ulceration. Regarding the molecular conformations of the crystalline forms and the rates of inhibition of stress ulceration, the *gauche* orientation of the guanidine group relative to the imidazole ring would be the conformation necessary for effective binding to the histamine H_2-receptor. The compactly folded conformation of form C appears to be optimal for binding to the active site of the receptor and for clinical efficacy.

Keyphrases □ Cimetidine—polymorphic crystalline forms, X-ray structural studies, physicochemical properties □ Polymorphism—cimetidine crystals, X-ray structural studies, physicochemical properties □ Structure—polymorphic crystalline forms of cimetidine, X-ray studies, physicochemical properties

Cimetidine, *N″*-cyano-*N*-methyl-*N′*-[2-[[(5-methyl-1*H*-imidazol-4-yl)methyl]thio]ethyl]guanidine, a specific competitive histamine H_2-receptor antagonist, inhibits the secretion of histamine-stimulated gastric acid. Because of its minimal side effects, it is widely used in the treatment of human peptic ulcers (1). Cimetidine has different crystalline forms (polymorphism) when crystallized under various conditions (2, 3). Since the bioavailability of

0022-3549/83/1200-1436$01.00/0

pharmacologically active compounds is generally dependent on their crystalline forms (4), detection of the most active among the cimetidine crystalline forms is important for understanding the specific stereochemistry of the H_2-receptor and for the effective clinical use of the agent.

This paper reports the physicochemical properties of four cimetidine crystalline forms (A, B, C, and D) obtained from aqueous solutions at different sample concentrations. The different forms were characterized by determining melting points, IR spectra, X-ray powder patterns, thermal behavior, and dissolution rates. The crystal structures of forms C and D were determined by X-ray diffraction.

EXPERIMENTAL

Preparation of Cimetidine Crystalline Forms—The preparation of the crystalline forms of cimetidine has been reported previously (3); crystallization from organic solvents such as acetonitrile produced platelet crystals, and crystallization from aqueous solutions produced three crystalline forms. Four crystalline forms were obtained by slow evaporation of the aqueous solutions; these were platelet (form A), needle (form B), pyramidal (form C), and cubic (form D) crystals. The cimetidine concentrations used for the preparation of crystal forms A, B, C, and D were 80, 10–40, 150, and 2–10 mg/ml, respectively[1]. The solutions were placed inside covered beakers and allowed to evaporate slowly at room temperature (25°; forms A, B, and D) or at 4–6° (form C). After 3–4 weeks, well-formed crystals were obtained; the crystalline forms were confirmed to coincide with those reported previously (3) by comparison of their respective IR spectra.

IR Spectra and Thermal Analyses—IR spectra were measured by using potassium bromide disks[2]. Gravimetry and the calorimetric changes accompanying the thermal decomposition were measured by thermogravimetry (TG) and differential thermal analysis (DTA) instruments[3]. The TG and DTA profiles were measured using 20 mg of powdered samples; the heating rate was 5°/min.

X-ray Powder Patterns—X-ray powder patterns were measured by the permeance method, using a diffractometer[4] and copper Kα radiation. The powder pattern of each crystalline form was measured twice and averaged.

X-ray Data Collection of Crystalline Forms C and D—Preliminary oscillation and Weissenberg photographs showed both crystal systems to be monoclinic (Table I). The density of both crystals was measured by the flotation method in benzene–carbon tetrachloride. A single crystal (0.3 × 0.3 × 0.4 mm, form C; 0.5 × 0.4 × 0.3 mm, form D) was mounted on a computer-controlled four-circle diffractometer[5]. Intensity data on 2305 (form C) and 2138 (form D) independent reflections [$Fo \geq 3\sigma(Fo)$] were obtained using graphite-monochromated copper Kα radiation and the $\omega - 2\theta$ scanning technique ($\sin\theta/\lambda \leq 0.588$ Å^{-1}). The scan speed was 4°/min; the background was measured for 5 sec. The intensity of four standard reflections for the respective crystals, measured every 100 reflections, showed no structural deteriorations due to X-ray irradiation during the measurement of all reflections. Corrections were applied for the Lorentz and polarization factors, but not for the absorption effects.

Structure Determinations and Refinements—The structures of forms C and D were solved by the direct method using the MULTAN 78 program (5). An electron density map using the normalized structure factors (E), computed with the phase set having the highest figure of merit using 180 reflections with $|E| \geq 1.57$ (form C) or 170 reflections with $|E| \geq 1.73$ (form D), gave reasonable positions for all nonhydrogen atoms. The atomic coordinates were refined by the block-diagonal least-squares method with anisotropic temperature factors. The positional parameters of all hydrogen atoms could be determined from a difference Fourier map.

Refinement, including those parameters with isotropic temperature factors, was then continued. The quantity minimized was $\Sigma\omega(|Fo| - |Fc|)^2$; in the final refinement, the following weighting scheme was used: for form C, $w = 0.24$ for $Fo = 0.0$, $w = 1.0$ for $0 < Fo \leq 11.0$, and $w = 1.0/[1.0 + 0.112(Fo - 11.0)]$ for $Fo > 11.0$; for form D, $w = 1.0$ for $0 < Fo \leq 9.0$ and $w = 1.0/[1.0 + 0.235(Fo - 9.0)]$ for $Fo > 9.0$. The final R-value was 0.049 for form C and 0.039 for form D.

The final atomic positional and thermal parameters of form D are given in Tables II and III, respectively[6]. All numerical calculations were performed using the UNICS programs (6)[7]. Atomic scattering factors cited in the *International Tables for X-ray Crystallography* (7) were used.

Measurement of Dissolution Rates of the Four Crystalline Forms in Deionized Water—A schematic drawing of the dissolution apparatus is presented in Fig. 1. Deionized water (46 ml) was introduced into the dissolution chamber outside the cellulose dialysis membrane.[8] Each crystalline form (20 mg, 44–74 μm in diameter), suspended in 4 ml of

Table I—Crystal Data

	Crystalline Form	
	Form C	Form D
	$C_{10}H_{16}N_6S{\cdot}H_2O$	$C_{10}H_{16}N_6S$
Molecular weight	270.35	252.34
Crystal system	Monoclinic	Monoclinic
Space group	Cc	$P2_1/n$
Cell constants		
a(Å)	12.620(5)	7.284(1)
b(Å)	7.772(4)	10.814(2)
c(Å)	14.742(5)	16.172(3)
β(°)	117.76(2)	94.69(1)
V(Å^3)	1342.8(1)	1269.5(4)
Z	4	4
Dm(g·cm^{-3})	1.333(1)	1.310(1)
Dx(g·cm^{-3})	1.337	1.320
μ(Cu-Kα) (cm^{-1})	20.919	21.175
F(0 0 0)	576	536

Table II—Atomic Coordinates of Form D

Atom	x^a	y^a	z^a
S	0.7407(1)	0.7499(0)	0.7395(0)
N(1)	0.5812(2)	0.4240(1)	0.9221(1)
N(2)	0.7377(2)	0.5961(2)	0.9112(1)
N(3)	0.6810(2)	0.6042(1)	0.5648(1)
N(4)	0.5043(2)	0.7121(1)	0.4654(1)
N(5)	0.3763(2)	0.6333(2)	0.5834(1)
N(6)	0.0580(2)	0.6768(2)	0.5290(1)
C(1)	0.7292(3)	0.4908(2)	0.9504(1)
C(2)	0.5861(2)	0.5969(2)	0.8537(1)
C(3)	0.4889(3)	0.4904(2)	0.8597(1)
C(4)	0.3176(3)	0.4432(2)	0.8136(2)
C(5)	0.5465(3)	0.7011(2)	0.7952(1)
C(6)	0.8324(2)	0.6043(2)	0.7072(1)
C(7)	0.7131(2)	0.5349(2)	0.6415(1)
C(8)	0.5185(2)	0.6513(2)	0.5374(1)
C(9)	0.6488(3)	0.7192(2)	0.4096(1)
C(10)	0.2102(2)	0.6590(2)	0.5514(1)
H(N1)	0.540(3)	0.351(2)	0.940(2)
H(N3)	0.775(2)	0.623(2)	0.540(1)
H(N4)	0.412(3)	0.753(2)	0.453(1)
H(1)	0.815(3)	0.468(2)	0.995(1)
H(4a)	0.294(5)	0.490(3)	0.768(2)
H(4b)	0.221(5)	0.423(3)	0.848(2)
H(4c)	0.339(5)	0.364(4)	0.783(3)
H(5a)	0.440(3)	0.676(2)	0.754(1)
H(5b)	0.514(3)	0.775(2)	0.824(1)
H(6a)	0.859(3)	0.550(2)	0.759(1)
H(6b)	0.952(3)	0.631(2)	0.686(1)
H(7a)	0.591(3)	0.515(2)	0.661(1)
H(7b)	0.778(3)	0.460(2)	0.627(1)
H(9a)	0.596(4)	0.757(2)	0.359(2)
H(9b)	0.699(3)	0.637(2)	0.398(1)
H(9c)	0.749(3)	0.766(2)	0.431(1)

[a] *SD* in parentheses.

[1] The reproducibilities of forms A, B, and C were very good, but that of form D could not be warranted.
[2] Model 260-10, Hitachi infrared spectrometer, Japan.
[3] Model M8075, Rigaku Denki Co., Japan.
[4] Microflex, Model 4180D1, Rigaku Denki Co., Japan.
[5] Model AFC-5, Rigaku Denki Co., Japan.

[6] After the present determination and refinements of the form C crystal, an independent determination of this crystal form was reported by B. Prodic-Kojic and Z. Ruzic-Toros (10). Their structure is identical to ours; however, their crystal parameters are somewhat different.
[7] These calculations were carried out on an ACOS-700 computer at the Computation Center of Osaka University.
[8] VisKing tube, Union Carbide Co.

Table III—Anisotropic Thermal Parameters ($\times 10^4$) of the Nonhydrogen Atoms of Form D[a]

Atom	B_{11}	B_{22}	B_{33}	B_{12}	B_{13}	B_{23}
S	259(1)	78(0)	32(0)	−86(1)	30(1)	−2(0)
N(1)	157(3)	73(1)	36(1)	−37(3)	32(2)	3(2)
N(2)	194(3)	86(2)	31(1)	−62(4)	13(2)	−8(2)
N(3)	114(2)	81(1)	25(1)	18(3)	8(2)	5(1)
N(4)	123(3)	80(1)	28(1)	27(3)	4(2)	12(1)
N(5)	122(3)	91(1)	30(1)	9(3)	19(2)	−2(1)
N(6)	120(3)	104(2)	56(1)	15(4)	34(2)	8(2)
C(1)	194(4)	99(2)	33(1)	−38(4)	9(3)	4(2)
C(2)	176(3)	74(2)	28(1)	−31(4)	32(2)	−14(2)
C(3)	173(4)	75(2)	31(1)	−19(4)	29(2)	−18(2)
C(4)	220(5)	115(2)	50(1)	−98(5)	−15(3)	−12(3)
C(5)	213(4)	79(2)	38(1)	−2(4)	35(3)	1(2)
C(6)	157(3)	107(2)	28(1)	7(4)	5(2)	10(2)
C(7)	171(3)	74(2)	29(1)	32(4)	−1(2)	11(2)
C(8)	116(3)	58(1)	25(1)	2(3)	3(2)	−13(1)
C(9)	157(3)	107(2)	27(1)	−9(4)	16(2)	13(2)
C(10)	140(3)	68(1)	35(1)	2(3)	42(2)	−6(2)

[a] The anisotropic temperature factors are expressed in the form: $\exp[-(B_{11}h^2 + B_{22}k^2 + B_{33}l^2 + B_{12}hk + B_{13}hl + B_{23}kl)]$. *SD* in parentheses.

deionized water, was introduced into the membrane. The test solution (550 ml) was placed into the reservoir; the total aqueous solution for measuring the dissolution rate constants was maintained at a volume of 600 ml, in order to retain the sink condition ($C \ll C_s$, where C is the concentration of the used sample and the C_s is the saturated sample).

The dissolution chamber was shaken at 200 strokes/min in an incubator at 37 ± 0.5°. The aqueous solution was circulated with a pump at a flow rate of 9.0 ml/min; the dissolved amount of the drug as a function of time was continuously monitored using a UV spectrophotometer (220 nm).

In addition to this method, the dissolution rate constants of forms A, B, and C were measured by the rotating disk method. These samples were tentatively measured using the compressed disks under several pressures: 454, 908, 1362, 1816, and 2270 kg/cm^2. As the rates of these forms were almost unchanged within the range of 454–2270 kg/cm^2, the experiment was carried out under the pressure that was suitable for making disks. The preparation of the disk samples did not affect the crystalline forms until a pressure of 4540 kg/cm^2 was reached, as verified by IR spectra.

All experiments were carried out under the following conditions. The compressed disk was attached to a holder of matched size in such a manner that only the bottom face of the disk was in contact with the deionized water; the other part of the disk was covered with paraffin. The holder (with disk) was attached to the shaft and set in a flask containing 1000 ml of deionized water; the flask was placed in a constant temperature bath (37 ± 0.5°). The rotating velocity of the disk was 100 rpm. The dissolved amount of the sample was monitored as noted above.

RESULTS AND DISCUSSION

Melting Points and IR Spectra of Four Crystalline Forms—The melting points of the four crystalline forms and their characteristic IR bands are summarized in Table IV. The IR spectra of crystalline forms A, B, C, and D corresponded to forms I, IV, II, and III reported by Pro-

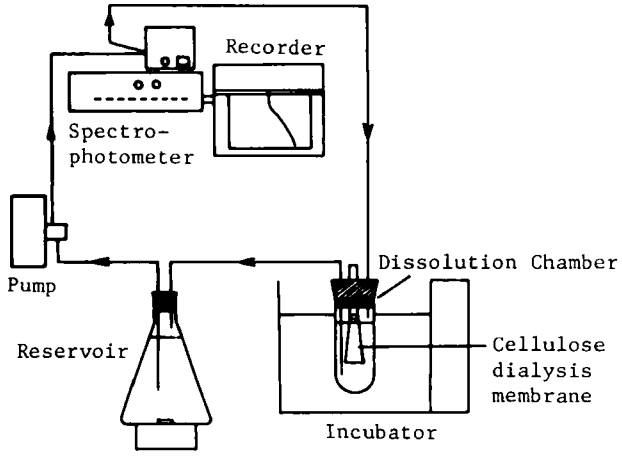

Figure 1—*Schematic drawing of the dissolution apparatus.*

Table IV—Melting Points and IR Spectra of the Four Crystalline Forms

Form	Crystal Form	Melting Point	Characteristic bands, cm^{-1}
A	plate	149–152°	1210 1160 1025 800 765 758 690 670 605 560 540
B	needle	152–154°	2850 1430 1420 1220 1190 1120 1040 650 630 590
C	pyramid	81–83°	3510 3400 3300 1180 1170 1130 1110 880 870 605 470
D	cube	146–147°	3400 3000 2920 2850 1470 1210 1190 1180 1160 1035 515 480

dic-Kojic *et al.* (3). Form C had the characteristic band at 3510 cm^{-1} corresponding to the hydroxyl group; its melting point was lower than that of the other forms, suggesting the presence of water of crystallization. The other crystalline forms, with melting points higher than form C, were anhydrous forms, indicative of the crystalline polymorphism of cimetidine. This point was also confirmed by measuring the X-ray powder patterns (Fig. 2).

DTA and TG Profiles—Figures 3 and 4 show the DTA and TG profiles of the four crystalline forms. In these profiles, the DTA and TG curves represent the thermal change and the percent of weight loss, respectively. In the DTA curves of forms B and D (Fig. 3), the endothermic peaks near 150° corresponded to the respective melting points. Exothermic reactions began near 185°. Although the thermal change behavior was similar, form D appears to be more loosely packed within the crystalline lattice because its endo- and exothermic peaks were smaller than those of form B. This idea is also supported by the difference of their densities [Dm = 1.351(2) g·cm^{-3} for form B and Dm = 1.310(1) g·cm^{-3} for form C].

In the DTA curve of form A (Fig. 4), the endothermic peak near 150° was larger than that of forms B and D. As is obvious from the TG curve below 150°, form A crystal is thermally quite stable; decomposition begins at a temperature >200°. These data suggest that the molecular packing mode of form A is thermodynamically more stable than that of forms B and D.

On the other hand, the DTA and TG curves of form C were very different; there were two endothermic peaks near 80° and 150° in the DTA curve. In the TG curve at 80°, which corresponds to the melting point of this form, the weight loss of one water molecular per cimetidine molecule was observed. Above 80°, the DTA and TG curves of form C were identical to those of form A, suggesting that the structural change of form C to form A was due to the release of water of crystallization. This point was also confirmed by measuring the IR spectra and the X-ray diffraction patterns.

Molecular Structure of Cimetidine in Crystalline Form D—Figure 5 shows the bond lengths and angles of form D with their atomic num-

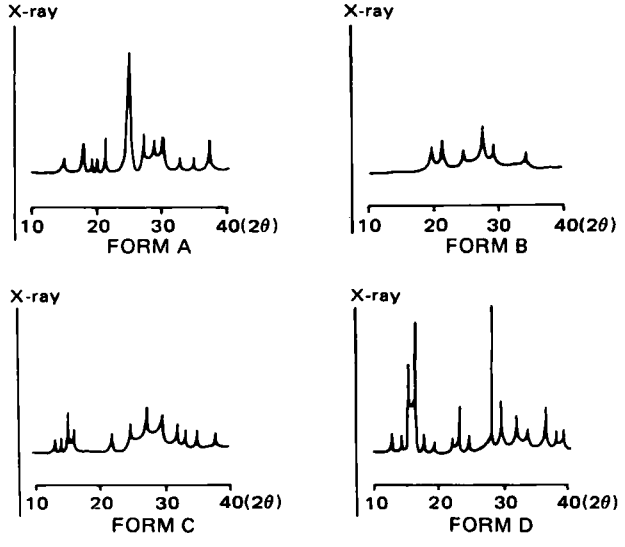

Figure 2—*X-ray powder patterns of the four crystalline forms (20°).*

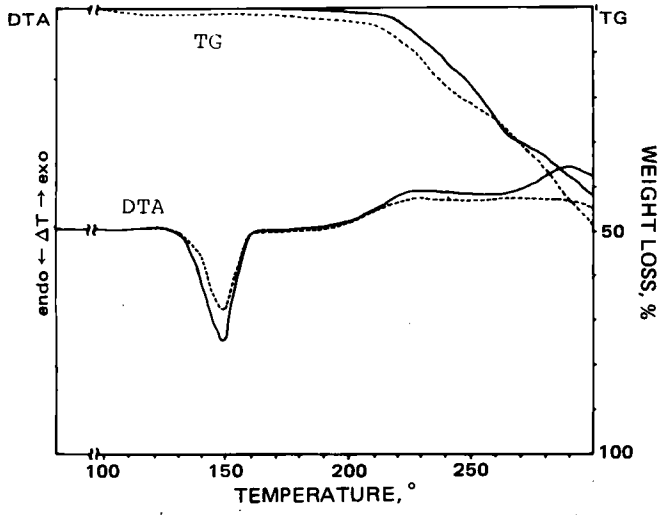

Figure 3—*Differential thermal analysis (DTA) and thermogravimetric (TG) curves of forms B (—) and D (- - - -).*

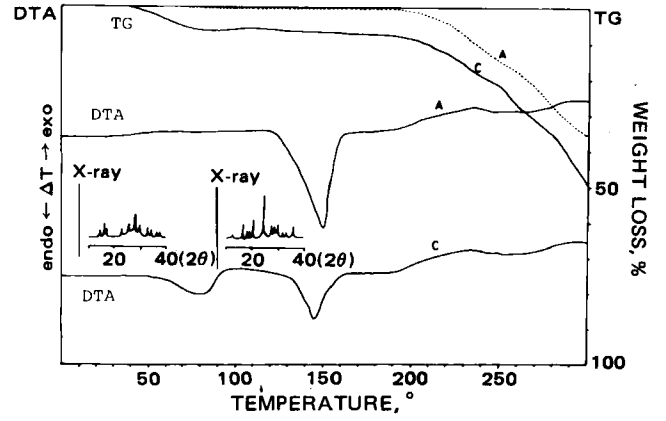

Figure 4—*Differential thermal analysis (DTA) and thermogravimetric (TG) curves of forms A and C. The X-ray powder patterns of form C and dehydrated form C on heating to 100° are also shown (insets).*

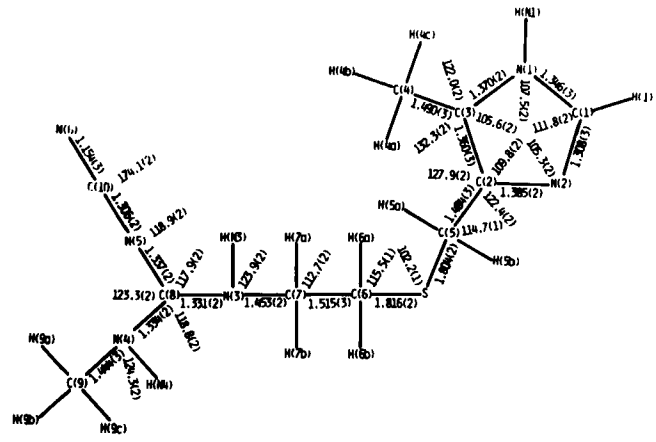

Figure 5—*Bond lengths (Å) and angles (°) of the nonhydrogen atoms of form D (with SD in parentheses).*

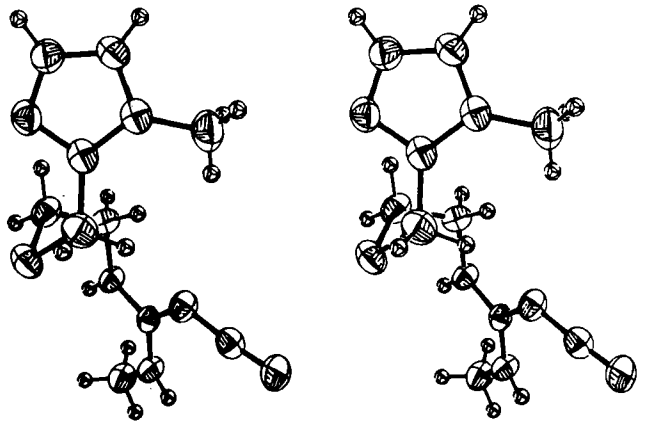

Figure 6—*Stereoscopic drawings of the molecular conformation of form D projected onto the imidazole ring.*

bering. The equations of the least-squares planes for the imidazole ring, C(2)—C(5)—S, S—C(6)—C(7)—N(3), and the guanidine group, the displacement of individual atoms from these planes, and the dihedral angles between the planes are listed in Table V. A stereoscopic drawing of the molecule, projected onto the imidazole ring, is presented in Fig. 6.

Although the observed bond angles were in agreement with those of related histamine H_2-receptor antagonists within their estimated standard errors, the bond length of the thioether linkage in form D, C(5)—S (1.804 Å), was significantly shorter than that of form A (1.828 Å) (8), form

Table V—Optimal Planes and Deviations (Å) of Individual Atoms

Equations of the best planes expressed by $m_1x + m_2y + m_3z = d$ in the orthogonal space

Plane	m_1	m_2	m_3	d
I Imidazole ring	0.60174	−0.43525	−0.66967	−10.13240
II C(2)C(5)S	0.20995	0.65007	0.73029	14.90376
III SC(6)C(7)N(3)	0.93047	0.26603	−0.23191	3.27256
IV Guanidine group	0.18502	0.85315	0.48775	10.79567

Deviations (Å) from the best plane

I Imidazole Ring		II C(2)C(5)S		III SC(6)C(7)N(3)		IV Guanidine Group	
C(1)*	0.004(3)	C(2)*	0.000(0)	S*	−0.008(1)	C(8)*	0.006(2)
C(2)*	−0.002(2)	C(5)*	0.000(0)	C(6)*	0.366(3)	N(3)*	−0.002(2)
C(3)*	0.003(2)	S*	0.000(0)	C(7)*	−0.295(2)	N(4)*	−0.002(2)
N(1)*	−0.003(2)	C(3)	−0.828(3)	N(3)*	0.093(2)	N(5)*	−0.002(2)
N(2)*	−0.004(2)	N(2)	0.888(4)	C(8)	−0.728(3)	C(7)	−0.014(3)
C(4)	0.009(4)	C(6)	−1.255(4)	C(5)	−1.759(2)	C(9)	−0.166(3)
C(5)	0.012(3)					C(10)	−0.232(3)
H(1)	−0.030(23)					N(6)	−0.444(4)
H(N1)	−0.047(27)					H(N3)	0.106(19)
						H(N4)	0.153(20)

Dihedral angles (°) between the best planes

	II	III	IV
I	49.8(1)	52.2(1)	54.1(1)
II		79.4(1)	18.3(1)
III			74.0(1)

[a] Atoms with asterisks define the plane in each case.

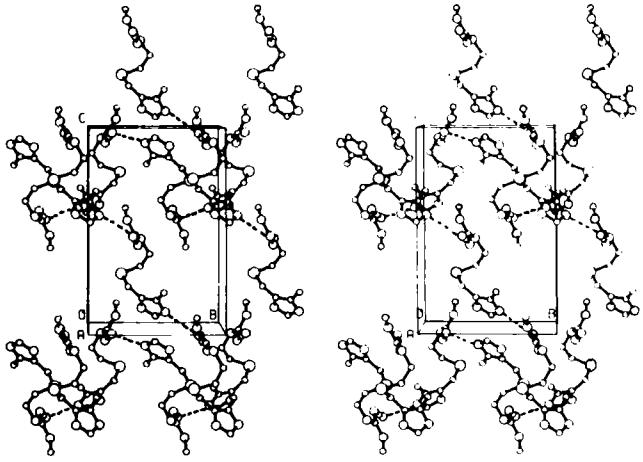

Figure 7—*Stereoscopic drawings of the molecular packing of form D, viewed along the* a*-axis. For the sake of clarity, the hydrogen atoms are omitted. The dotted lines represent the hydrogen bonds.*

C (1.825 Å), metiamide (1.828 Å) (9), and *N*-[2-[(imidazol-4-yl)methylthio]ethyl]-*N″*-methylthiourea (thiaburimamide) (1.829 Å) (9); the C(8)—N(5) bond length of the guanidine group (1.337 Å) is also shorter than that of form A (1.346 Å) and form C (1.343 Å). As in the related molecules, the imidazole ring of this crystal is planar with a maximum shift of 0.004 Å for the C(1) and the N(2) atoms; and C(4) and the C(5) atoms lie almost on this plane. The guanidine group is also planar with a maximum deviation of 0.006 Å for the C(8) atom; the C(7) atom lies essentially on the plane.

As is obvious from Fig. 6, the molecule can be characterized by its spiral-shaped conformation. The dihedral angle between the imidazole ring and the guanidine group is 54.1(1)°; both moieties are linked to each other by the C(5)—S—C(6)—C(7)—N(3) bond sequence manifesting the spirally curled arrangement with an ~360° rotation.

Crystal Packing of Crystalline Form D—The molecular packing viewed down the *a*-axis is shown in Fig. 7; the hydrogen bonding parameters and the short contacts <3.5 Å are listed in Table VI. The molecules are linked *via* intermolecular hydrogen bonds with the imidazole and guanidine nitrogen atoms of neighboring molecules, N(1)—H(N1)···N(6) = 2.988(2) Å and N(3)—H(N3)···N(6) = 2.959(2) Å, thereby forming head-to-tail molecular arrangements in the *b*- and *c*-directions. Many short contacts were observed between neighboring imidazole rings, between neighboring guanidine groups, and between the neighboring imidazole ring and guanidine group. These short contacts stabilize the molecular packing in the crystal.

Molecular and Crystal Structure of Form C—Since the present crystal determination showed the molecular and crystal structure of form C to be identical with that reported by Prodic-Kojic and Ruzic-Toros (10), the structural features observed in the crystal will be presented briefly. The molecular conformation in this crystal is characterized by the folded form resulting from the weak stacking interaction between the imidazole and guanidine moieties. The dihedral angle between both planes is 10.8(2)°; their mean interplanar spacing is 3.676 Å. This conformation is further stabilized by the hydrogen bond formed by the water of crystallization [N(1)···O = 2.383(7) Å, N(6)···O = 3.064(8) Å]. In the crystal packing, the water of crystallization is further hydrogen bonded to the N(2) atom of the neighboring imidazole ring [N(2)···O = 2.800 (7) Å]. The infinite double layers, found by these three hydrogen bonds by water of crystallization and a N(6)···N(3) hydrogen bond [3.034(8) Å], are arranged parallel to the *a*- and *b*-directions and are held together by van der Waals contacts in the *c*-direction.

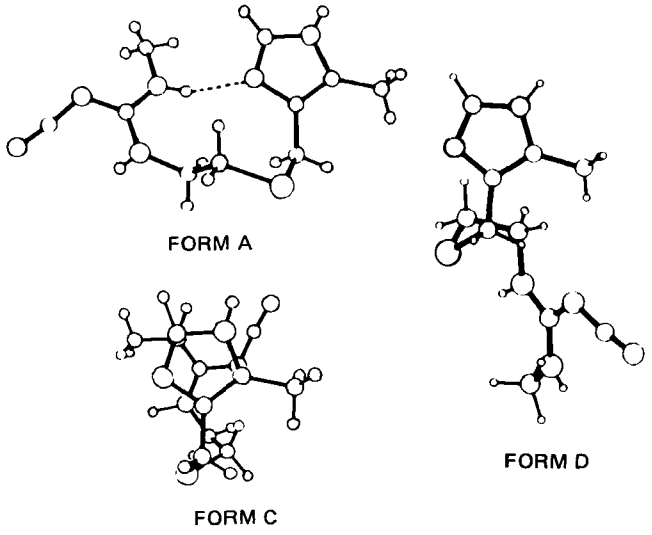

Figure 8—*Comparison of the molecular conformations of forms A, C, and D projected onto the imidazole ring.*

Table VII—Comparison of the Torsion Angle of the Cimetidine Molecule Observed in Crystalline Forms A, C, and D

	Form A	Form C	Form D
N(2)—C(2)—C(5)—S	−73.1	70.5(6)	49.4(2)
C(3)—C(2)—C(5)—S	108.3	−106.6(6)	−129.5(2)
C(2)—C(5)—S—C(6)	61.3	59.8(5)	−45.4(2)
C(5)—S—C(6)—C(7)	61.2	138.5(4)	69.2(2)
S—C(6)—C(7)—N(3)	184.3	68.6(5)	60.7(2)
C(6)—C(7)—N(3)—C(8)	92.1	76.2(7)	110.8(2)
C(7)—N(3)—C(8)—N(4)	−8.8	178.5(5)	−179.1(2)
C(7)—N(3)—C(8)—N(5)	172.6	−2.1(8)	−0.2(2)
N(3)—C(8)—N(4)—C(9)	171.8	1.0(9)	−7.2(3)
N(3)—C(8)—N(5)—C(10)	−12.5	175.5(5)	168.0(2)

Table VIII—Intramolecular Distances (Å) Between the N(2) Atom of the Imidazole Ring and the Nitrogen Atom of the Cyanoguanidine Group

	Form A	Form C	Form D
N(3)	4.090	3.914(7)	5.584(2)
N(4)	2.881	3.836(7)	7.378(2)
N(5)	5.061	4.416(8)	5.737(2)
Orientation between the imidazole ring and the cyanoguanidine group	*gauche*	*gauche*	*trans*

Molecular Conformations Observed in Forms A, C, and D and Their Biological Implications—The molecular conformations and selected torsion angles observed in the crystal structures of forms A, C, and D are presented in Fig. 8 and Table VII. Since forms A, C, and D were

Table VI—Hydrogen Bonds and Short Contacts <3.5 Å [a]

Donor(D)	Acceptor(A)	Distance, Å	Angle, °
		Hydrogen bonds	
N(1)	$N(6)^{I}$	D···A 2.998(2) H···A 2.08(3)	D—H···A 175(2)
N(3)	$N(6)^{II}$	D···A 2.959(2) H···A 2.17(2)	D—H···A 156(1)
		Short contacts (Å) < 3.5 Å	
$N(1)—N(1)^{III}$	3.306(3)	$N(3)—C(8)^{V}$	3.476(2)
$N(1)—C(1)^{III}$	3.312(3)	$N(4)—C(7)^{V}$	3.490(2)
$N(2)—N(4)^{IV}$	2.926(2)	$C(8)—C(8)^{V}$	3.492(2)
$N(2)—N(6)^{IV}$	3.432(2)	$C(9)—N(6)^{II}$	3.447(3)

[a] Roman numerals denote the following equivalent positions relative to the reference molecule at *x,y,z*: (I) 1/2 − *x*, −1/2 + *y*, 3/2 − *z*; (II) 1 + *x,y,z*; (III) 1 − *x*,1 − *y*,2 − *z*; (IV) 1/2 + *x*,3/2 − *y*,1/2 + *z*; (V) 1 − *x*,1 − *y*,1 − *z*. *SD* in parentheses.

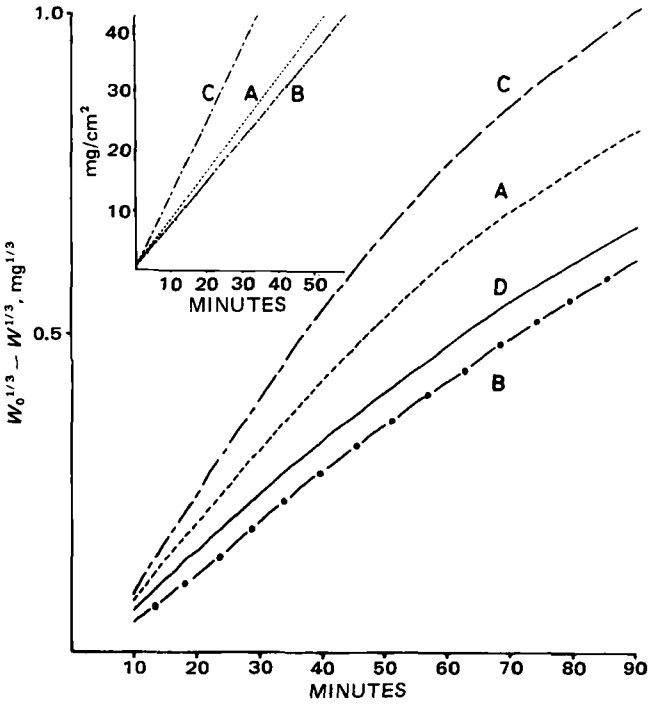

Figure 9—*Dissolution profiles of the four crystalline forms in particle systems and those of the three crystalline forms in disk systems (inset).*

prepared from aqueous solutions at different sample concentrations, the energetic stability of their molecular conformations (Fig. 8) appears to be the same. The conformations of forms A, C, and D are characterized by an intramolecular hydrogen bond formation, leading to the formation of a stable 10-member ring (form A), by a weak stacking interaction between the imidazole and guanidine moieties which is further stabilized by the hydrogen bond formation by water of crystallization (form C), and by a spiral conformation (form D).

Based on extended Hückel molecular orbital calculations of various related agonists, Kier (11) proposed that the conditions necessary for the H_2-receptor activity of histamine are: (*a*) distance between the N(2) atom of the imidazole ring and the nitrogen atom of the side chain is near 3.6 Å and (*b*) the orientation of the nitrogen atoms with respect to the imidazole ring is *gauche*. Durant *et al.* (12) reported that the introduction of an unchanged side chain such as the cyanoguanidine group into the imidazole ring is more effective for binding to the histamine H_2-receptor.

Table VIII lists the intramolecular distances between the N(2) atom of the imidazole ring and the N(3), N(4), or N(5) atom of the cyanoguanidine group, and the orientation between the two moieties in the cimetidine molecules. The *gauche* orientation of the guanidine group with respect to the imidazole ring is observed in forms A and C; their intramolecular N—N distances are in the range of 2.881–5.061 Å for form A and 3.836(7)–4.416(8) Å for form C. On the other hand, form D takes a *trans* orientation; the distance in this form ranges from 5.584(2) to 7.378(2) Å. According to the proposal of Kier (11), the molecular conformation of form A or C would probably be the conformation necessary for effective binding to the histamine H_2-receptor. The conformation of form C, which has an N—N distance of ~3.6 Å and *gauche* orientation, appears to be the most highly preferred conformation for binding to the active site of the receptor, although the energetically stable 10-member ring of form A, effected by an intramolecular hydrogen bond, was also found in the related H_2-receptor antagonists, metiamide (9) and *N*-[4-(imidazol-4-yl)butyl]-*N'*-methylthiourea (burimamide) (13).

Table IX—Effects of Four Crystalline Forms for Stress Ulceration in Rats

Dose, mg/kg	Mean Area of Ulcer, mm^2	Inhibition Rate, %
Control	22.3 ± 4.3	
Form A		
12.5	6.9 ± 2.1	69.3
25.0	5.9 ± 2.4	73.7
50.0	3.4 ± 2.3	84.4
Form B		
12.5	8.7 ± 4.8	60.8
25.0	3.2 ± 1.1	85.5
50.0	3.6 ± 2.2	84.0
Form C		
12.5	2.8 ± 1.7	87.4[a]
25.0	3.2 ± 1.1	85.8
50.0	2.2 ± 0.9	90.4
Form D		
12.5	8.0 ± 2.6	64.1

[a] $p < 0.05$ relative to the same dose of form A or B.

Dissolution Rates of the Four Crystal Forms and Their Efficacy in Preventing Stress Ulceration—The dissolution profiles measured by disk and particle methods are shown in Fig. 9. The rotating disk preparation was carried out under a pressure of 1362 kg/cm^2. The dissolution rate constants of forms A, B, and C were 0.81(6), 0.74(4), and 1.24(6) mg/cm^2/min, respectively; that of form C is ~1.53 and 1.68 times greater than those of forms A and B[9]. In the particle system, the dissolution rate can be expressed in terms of the Hixson–Crowell law (14), $W_0^{1/3} - W^{1/3} = Kt$, where W_0 is the initial weight of drug, W is the undissolved weight at time t, and K is the apparent dissolution rate constant. Up to 40 min, the profiles appear to be linear, suggesting that application of the Hixson–Crowell law is valid for measuring the dissolution rate of cimetidine. The dissolution rate constants of form A, B, C, and D during the 40-min period were 1.16(4), 0.79(1), 1.50(5), and 0.88(6) × 10^{-2} $mg^{1/3}$/min, respectively. The rate constant for form C is ~1.29, 1.70, and 1.90 times greater than those for forms A, D, and B, respectively. The results obtained by these two different methods show clearly that form C is more soluble in deionized water than the other forms. This relationship has also been observed in the difference of their solubilities [5.4(1), 4.7(1), 5.8(1), and 5.0(1) g/liter for forms A, B, C, and D, respectively, at 25°] and in gastric juice[10].

The effect of the four crystalline forms on rat gastric ulcers produced by restraint and water-immersion stress was also examined[11]. The animals received a peroral dose of 12.5, 25.0, or 50.0 mg/kg of the respective crystalline form before water immersion. The inhibition rate of the drug on the development of stress ulcers was calculated as follows:

$$\text{Inhibition rate (\%)} = 100 \times \frac{Mc - Mt}{Mc}$$

where Mc is the mean of the total ulcer area for rats in the control group (n = 12) and Mt is the mean of the total ulcer area in the test groups (n = 6/crystalline form). The Student's t test was used to determine the statistical significance of data obtained in this study. The results are given in Table IX; full details of this experiment will be reported elsewhere. Form C, especially at the lower dose which corresponds to that used clinically, exhibited significant inhibition of stress ulceration; results of the t test at the 12.5-mg/kg dose showed that form C was significantly more effective than forms A, B, and D.

REFERENCES

(1) R. N. Brogden, R. C. Heel, T. M. Speight, and G. S. Avery, *Drugs*, **15**, 93 (1978).

(2) Smith Kline & French, *German Patent Application*, 2742531 (1978).

(3) B. Prodic-Kojic, F. Kajfes, B. Belin, R. Toso, and V. Sunjic, *Gazz. Chim. Ital.*, **109**, 535 (1979).

(4) J. K. Haleblian, *J. Pharm. Sci.*, **64**, 1269 (1975).

(5) P. Main, S. E. Hull, L. Lessinger, G. Germain, J. P. Declerq, and M. M. Woolfson, "A System of Computer Programs for the Automatic Solution of Crystal Structures from X-ray Diffraction Data, MULTAN 78," University of York, England, 1978.

(6) "The Universal Crystallographic Computing System," Library of Programs, Computing Center of Osaka University, Osaka, Japan, 1979.

(7) "International Tables for X-ray Crystallography," vol. IV, Kynoch Press, Birmingham, England, 1974.

[9] The experiment for form D was omitted because of the difficulty in preparing its crystalline form.

[10] H. Kokubo, M. Shibata, K. Morimoto, K. Morisaka, T. Ishida, and M. Inoue, unpublished data.

[11] The inhibition of stress ulceration of form D was examined with only one dose (12.5 mg/kg) because large-scale preparation of this form was very difficult.

(8) E. Hädicke, F. Frickel, and A. Franke, *Chem. Ber.*, 111, 3222 (1978).
(9) K. Prout, S. R. Critchley, C. R. Ganellin, and R. C. Mitchell, *J. Chem. Soc. Perkin Trans. II*, **1977**, 68.
(10) B. Prodic-Kojic and Z. Ruzic-Toros, *Acta Crystallogr.*, **B36**, 1223 (1980).
(11) L. B. Kier, *J. Med. Chem.*, **11**, 441 (1968).
(12) G. J. Durant, C. R. Ganellin, and M. E. Parsons, *J. Med. Chem.*, **18**, 905 (1975).
(13) B. Kamenar, K. Prout, and C. R. Ganellin, *J. Chem. Soc. Perkin Trans. II*, **1973**, 1734.
(14) A. Hixson and J. Crowell, *Ind. Eng. Chem.*, **23**, 923 (1931).

Volume Shifts and Protein Binding Estimates using Equilibrium Dialysis: Application to Prednisolone Binding in Humans

THOMAS N. TOZER, JOHN G. GAMBERTOGLIO ˣ, DANIEL E. FURST, DENIS S. AVERY, and NICHOLAS H. G. HOLFORD

Received November 19, 1981, from the *Schools of Pharmacy and Medicine, University of California, San Francisco, CA 94143.* Accepted for publication October 21, 1982.

Abstract □ Sizable volume shifts can occur during equilibrium dialysis. This net movement of water, presumably caused by the osmotic effect of plasma proteins, reduces the concentration of binding proteins. In this paper the theory of protein binding estimation is extended, equations are developed for calculating the unbound and bound drug concentrations at dialysis equilibrium by correcting for the dilution of the proteins, and the equations are applied to a study of prednisolone. To demonstrate the importance of correcting for the volume shift, the parameters of a model in which prednisolone binds to corticosteroid-binding globulin, a protein with a limited capacity, and albumin were estimated. Unbound and bound concentrations were determined by correcting for both volume shifts (average 31%) and loss of drug to the buffer side, by correcting only for loss of drug to buffer side, and by making no correction at all (the usual method of treating equilibrium dialysis data). The error introduced by neglecting volume shifts was analyzed by comparing the parameter values obtained using the three methods. The results confirm the need to adjust for volume shifts and imply that reported binding constants obtained by equilibrium dialysis may be in error for many substances.

Keyphrases □ Equilibrium dialysis—measurement of protein binding, effect of volume shifts, theoretical model, application to prednisolone in humans □ Protein binding—determined by equilibrium dialysis, effect of volume shifts, theoretical model, application to prednisolone in humans □ Prednisolone—protein binding as determined by equilibrium dialysis, effect of volume shifts, application of theoretical model, humans

Binding of drugs to plasma proteins is important in pharmacokinetics and pharmacodynamics. Equilibrium dialysis is commonly employed for estimation of binding, but it has limitations. With the introduction of translucent cells, it has become evident that sizable volume shifts occur across the dialysis membrane. We have investigated the importance of these volume shifts in the estimation of plasma protein binding parameters and have developed a procedure to correct for them. The procedure is applied to a study of prednisolone in humans.

The binding of prednisolone in plasma is thought to involve two proteins, corticosteroid-binding globulin (transcortin) and albumin. In the range of concentrations associated with therapy (1), the plasma protein binding of prednisolone is concentration dependent largely because of saturable binding to sites on corticosteroid-binding globulin. It has been shown *in vitro* that glucocorticoid activity is a function of unbound concentration and that the activity can be altered by the addition or removal of the globulin (2). Definition of concentration–effect relationships for prednisolone, therefore, requires the ability to estimate unbound prednisolone concentrations. Estimates of unbound concentration *in vivo* can be obtained by measurement of total prednisolone concentration (bound plus unbound) and application of a suitable model for predicting the unbound concentration from the total concentration.

There are several complications in the use of equilibrium dialysis to estimate plasma protein binding. These include binding of drug to the dialysis cell or membrane, transfer of substantial amounts of drug from the plasma to the buffer side of the membrane, and osmotic volume shifts of fluid to the plasma side. Some of these problems have been discussed elsewhere (3). In this paper, a method is described for calculating the magnitude of osmotic volume shifts and for estimating the parameters that reflect binding *in vivo*.

THEORETICAL

Figure 1 is a schematic representation of equilibrium in a dialysis device containing plasma on one side and buffer solution on the other, with and without a volume shift. The volume of the plasma side is increased and the buffer side is decreased, because of a net osmotic transfer of water across the membrane. Osmotic equilibrium may or may not be reached at the time equilibrium is virtually achieved with respect to the drug. The derivations which follow assume conservation of the mass of prednisolone in the system and of the total volume of the two half-cells. Symbols and abbreviations are defined in Appendix I.

Conservation of Volume—The total volume of the cell is unchanged by dialysis; therefore:

$$\underset{\text{(before)}}{V_P + V_B} = \underset{\text{(after)}}{V'_P + V'_B} \qquad \text{(Eq. 1)}$$

Letting δ be the fractional increase in V_P due to osmotic water shift, then:

$$V'_P = V_P(1 + \delta) \qquad \text{(Eq. 2)}$$

and

0022-3549/83/1200-1442$01.00/0